SAND2017-8373C

Impact of Communication Latencies and Availability on Droop-Implemented Primary Frequency Regulation

Felipe Wilches-Bernal, Ricky Concepcion, and Raymond H. Byrne
Sandia National Laboratories
Albuquerque, NM 87185
{fwilche, rconcep, rhbyrne}@sandia.gov

***Abstract*—This paper proposes a method to modulate the power output of converter interfaced generators (CIGs) according to frequency variations. With the proposed approach, CIGs can successfully engage in the primary frequency regulation of a power system. The approach is a variation on the traditional droop-like proportional controller where the feedback signal is a global frequency measurement instead of a local one. Obtaining the global measurement requires transferring data using communications. This paper analyzes the performance of the proposed approach with respect to communications issues such as latencies and data dropouts. The approach implemented and tested in a simulation environment is compared against a method entirely based on local information. The results show that using global information in droop control provides benefits to the system as it improves its frequency regulation. The results also indicate that the proposed approach is robust to latencies and communication failures.**

***Index Terms*—Primary frequency response, photovoltaics, smart grid, droop, communication latencies**

I. Introduction

The advent of renewable energy sources such as solar and wind is changing the traditional configuration and operation of power systems. Solar and wind energy generation differ from conventional generation (coal, gas, hydro) units in that they are interfaced with the grid through power electronics converters which tend to reduce the inertia available in the system [1], [2]. Typically these types of sources do not participate in the frequency regulation of the system. These facts intensify system vulnerabilities to power imbalances, as the penetration of converter interfaced generators (CIGs) is increased. To mitigate these effects, it has been proposed that wind farms and/or solar plants engage in some form of frequency control [3]–[7]. The results of these works show that implementing frequency responsive controllers to converter interfaced generation is helpful to the frequency regulation of the system.

F. Wilches-Bernal, R. Concepcion, and R.H. Byrne are with Sandia National Laboratories. This research was supported by the U.S. Department of Energy, SunShot Initiative, under Agreement No. 30690. Sandia National Laboratories is a multimission laboratory managed and operated by National Technology and Engineering Solutions of Sandia, LLC., a wholly owned subsidiary of Honeywell International, Inc., for the U.S. Department of Energy's National Nuclear Security Administration under contract DE-NA0003525.

In power systems, primary frequency regulation is provided by the droop speed control included in certain synchronous machines throughout the system. This controller is simply a proportional action that adjusts the mechanical power input of the generator based on imbalances in the rotor speed. Controllers of this nature have been proposed for converter-interfaced energy resources to mitigate the negative effects that integrating these type of resources have on the frequency response of the system [3], [7], [8]. Because generating units from converter interfaced generators tend to be smaller in size and more dispersed geographically than conventional plants such as nuclear units, there is an opportunity to explore distributed control alternatives to tackle traditional power system problems using them as actuators [9]–[11]. In this paper, a droop-like controller for converter interfaced generation is proposed for these devices to participate in the frequency response of the system. In the proposed approach the controller uses a global frequency signal to determine the fluctuations in system frequency. This global signal is constructed from a weighted average of local frequencies. Because the controller needs system-wide information it is assumed communication infrastructure is in place.

The remainder of this paper is organized as follows. Section II presents the proposed droop control. Section III introduces the test system and conditions used to assess the proposed control approach. Section IV studies how the controller performs with variations in the control gain. Sections V and VI evaluate, respectively, the impact of communications time delay and availability on the controller performance. Finally, Section VII presents the conclusions of the work.

II. Communication Enabled Droop

Frequency needs to be kept within a tight range of the nominal value for power systems to operate adequately. The real-time control action that ensures frequency fluctuations are always within an acceptable range is the primary frequency regulation of the system determined by a droop governing action installed in defined generating units in the system. This control law is a proportional action described by

$$\Delta P_j = \frac{(f_{\rm ref} - f_{\rm eq})}{R} = k_R(f_{\rm ref} - f_{\rm eq}) \quad (1)$$

where $f_{\rm ref}$ is the nominal frequency (60 Hz in North America). The parameter R is known as the droop constant and is expressed as a percentage. k_R, which is the inverse of the droop, is used throughout this work. Traditionally, the droop controller is installed in synchronous generators and $f_{\rm eq}$ corresponds to the machine rotor speed. This feedback signal is hence a local signal.

The inclusion of CIG components to grid affects the frequency response of the system [1]–[3]. Power electronic interfaced generation reduces the total inertia available in the system and typically does not participate in frequency regulation. As a result, frequency response in the system is deteriorated with the inclusion of converter interfaced (CI) resources. To alleviate the deleterious effect of CIG integration to frequency regulation, a governing-like function like the one described in (1) is implemented in CIG devices. In such cases, $f_{\rm eq}$ is typically chosen as the frequency at the bus where the CIG device is installed. This frequency tends to be volatile and noisy as it is typically obtained from electrical quantities such as the phase angle of the voltage. In this work, a modification on the selection of $f_{\rm eq}$ is proposed and evaluated. The proposed signal to use is

$$f_{\rm eq} = \sum_{j=1}^{N} k_j f_j \quad (2)$$

as the feedback signal for the governing action of CI devices. Note that N is the total number of generators in the system and f_j is the rotor speed of the $j^{\rm th}$ machine. Hence the proposed signal is a weighted average of machine speeds and tends to smooth out the noisier and less relevant variations of local frequency measurements. Using this constructed measurement, effects such as local oscillations and inter-area oscillations are attenuated; only the global variation in frequency is retained. The weights k_j in 2 are defined as

$$k_j = \frac{H_j}{\sum_{i=1}^{N} H_i} \quad \text{for all} \;\; j \in \{1, \dots N\} \quad (3)$$

where H_j is the inertia constant of the $j^{\rm th}$ machine. In the proposed approach the feedback frequency signal is computed using system-wide machine speed information. It is then assumed that this information is transmitted from their location to a central entity, an aggregator, that computes the feedback signal and then transmits it to the CI devices. An alternative approach is to have each CI device compute the feedback signal which can be interpreted as a distributed implementation of the proposed approach. The mechanism of computation of the feedback signal is beyond the scope of this work which rather analyzes the advantages and disadvantages of using such type of signal. The proposed approach for governing control is referred to Communication-Enabled Droop (CE-Droop). This work evaluates the benefits of using such approach compared to the traditional droop approach based on local frequency measurements.

III. Test System and Solar Plant Model

In this work a reduced model of the Northeast Power Coordinating Council (NPCC) system was used to test the proposed CE-Droop approach. This model consist of 140 buses and 48 generators with a total of 28.042 GW of generation. The disturbance under consideration is the tripping of the Monroe generating unit in the Midwest region after 2 seconds of simulation. This event causes a loss of roughly 655 MW (nearly 2.3% of the total power production). The particular system under consideration is a version of the NPCC with approximately 50% solar photovoltaic (PV) penetration, obtained by substituting roughly half of the conventional generators with PV plants. The PV plants integrated into the system correspond to a custom model of a controlled current injection [9], [10]. The installation of the solar plants was performed evenly through all the geographic regions of the system. Note that the simulations of this work were performed in PSLF, a GE software platform widely used for power system analysis.

To analyze the frequency response variations with the proposed signal selection three main metrics are used. The first is the frequency nadir, f_N, which is the minimum frequency reached by system following the disturbance event. The second is the time to frequency nadir, t_{fN}, which is defined as the time taken by the system to reach the frequency nadir measured with respect to a defined reference (usually the start of the disturbance). The third one is the maximum separation of rotor angles which is used to analyze the transient stability of the system. This quantity is calculated by first computing the maximum rotor angle separation among all the generators in the system as a function of time $\theta_{\rm mx}(t)$ and then computing the maximum value taken by this function as

$$\Theta_{\rm max} = \max_{t \in [0, T_f]} (\theta_{\rm mx}(t)) \quad (4)$$

where T_f is the total time of the simulation.

IV. Effect of Variations in Droop Gain (k_R) on the Frequency Response

In this Section we present the effects of increasing the gain k_R to every PV plant in the system. Two scenarios are considered, one where each PV plant has a CE-Droop controller and another where the conventional droop (with local measurement only) is used. In the case of CE-Droop it is assumed that the global frequency information is available instantaneously (i.e. with no time delay). For each of this scenarios k_R was varied from 0 to 1000. For comparison, two more cases are studied: the no solar case and a case where the PV plants are not controlled (No control case) according to variations in frequency. Note that this latter case correspond to a controlled case with $k_R = 0$.

Fig. 1 (a) shows the frequency response of the system for the scenario where PV plants have conventional droop only

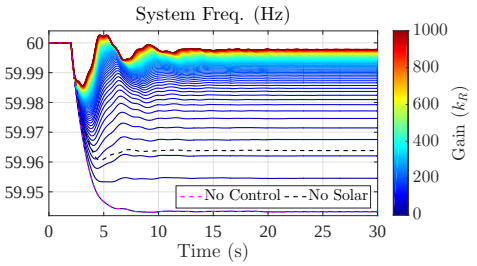

(a) Conventional droop.

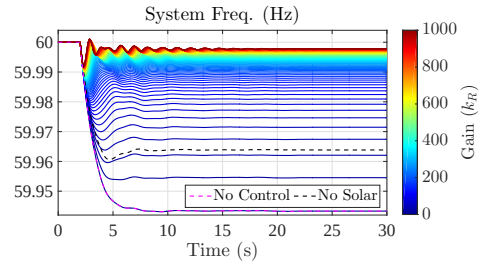

(b) CE droop.

Fig. 1: System frequency response for the loss of the Monroe generating unit. Comparison of conventional and communication enabled droop approaches.

and Fig. 1 (b) show the same results when the PV plants use the proposed CE-Droop approach. The no control case shows that including PV definitely deteriorates the frequency response of the system as both the frequency nadir and the settling frequency are lower than in the no solar case. The results in Fig. 1 also show that implementing either droop or the proposed CE-Droop to the PV plants in the system restores and even improves the frequency response of the system. As anticipated, higher gains tend to provide better results for both scenarios.

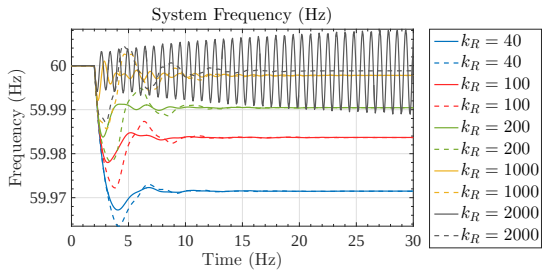

Fig. 2: Frequency responses of the system for different values of gain k_R. Solid lines show the results using the proposed CE droop approach while dashed lines show results with the conventional droop method.

Fig. 2 compares the conventional droop method against the proposed CE-Droop approach for $k_R = 40, 100, 200, 1000, 2000$. These results show that for the higher gain case ($k_R = 2000$) CE-Droop shows an undamped oscillation with a frequency of 1.31 Hz.

The frequency nadir of the system and the time the system takes to reach it were determined for the results in Fig. 1. These metrics were used to quantify the effect that increasing the value of k_R has on the frequency response of the system. Fig. 3a shows the variations in the frequency nadir of the system as a function of k_R for both the CE-Droop and conventional droop scenarios. These results show that the nadir is improved by increases in k_R. They also show that a small gain is enough to restore the nadir of the system from the solar no control case to the no solar case. Furthermore, these results reveal that for the same k_R value the resulting nadir using CE-Droop is always above the nadir when using the conventional droop. Regarding the time to frequency nadir metric, it is observed in Fig. 3b that CE-Droop also reaches the frequency nadir faster than the conventional droop approach for all levels of k_R. Combined, these results show that the frequency nadir of the system is enhanced using CE-Droop compared to using only conventional droop. The settling frequency of the system is also affected by k_R variations however there is no difference between the CE-Droop and conventional droop approaches as shown in Fig. 2.

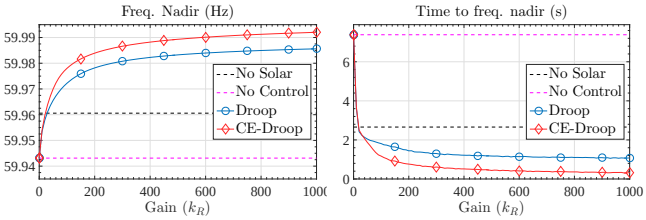

(a) f_N as a function of the gain k_R. **(b)** t_{fN} as a function of the gain k_R.

Fig. 3: Frequency nadir and the time it takes to reach it with variations in the effective gain k_R.

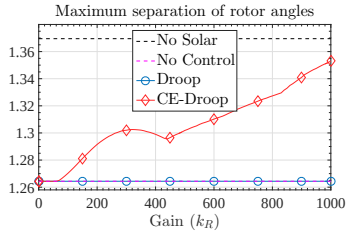

Fig. 4: Maximum rotor angle separation as a function of the gain k_R.

The maximum rotor angle separation as a function of gain k_R ($\Theta_{\max}(k_R)$) is presented in Fig. 4 for the CE-Droop and conventional droop methods. They show that $\Theta_{\max}$ is unaffected by changes in k_R when conventional droop is implemented while it mildly increases as k_R augments in the CE-droop scenario.

V. Effect of Variations in Time Delay (τ_d) on the Frequency Response

Computing the global frequency in equation (2) for the proposed CE-Droop approach is not instantaneous as it involves both the transfer of information and a computation processing time. The feedback signal f_{eq} then reaches each PV plant after a time lag. In this Section the effect of this time lag, noted τ_d,

is analyzed with the assumption that the delay experienced by each individual PV plant is the same[1].

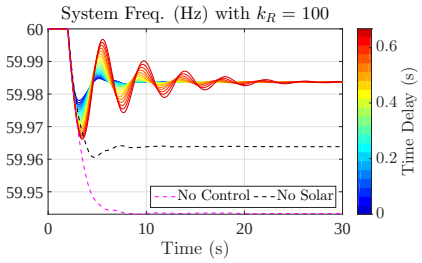

(a) CE-Droop gain $k_R = 100$.

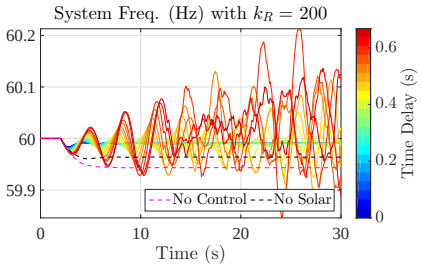

(b) CE-Droop gain $k_R = 200$.

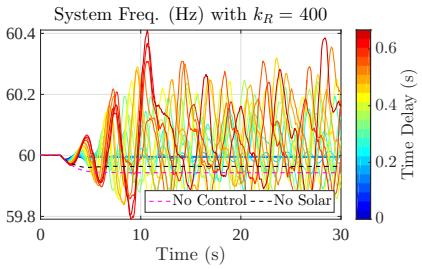

(c) CE-Droop gain $k_R = 400$.

Fig. 5: System frequency response for the loss of the Monroe generating unit. Comparison of the effect of time delay on CE-Droop for different gains values.

In Fig. 5 is observed how increments in the delay τ_d affect the frequency response of the system for k_R values of $100,\ 200,\ 400$. Fig. 5a presents the results when $k_R = 100$ which show that as τ_d increases, oscillations in the system start to appear. Results in Figs. 5 (a), (b), for k_R equal to 200 and 400 respectively, show that time delay values of 0.4 s and higher cause the system to lose synchronism.

The analysis of transient stability of the system was carried out using the maximum separation of rotor angles $\Theta_{\max}$. Fig. 6 shows variations in $\Theta_{\max}$ with increases in τ_d for different values of k_R as well as for the no control and no solar cases. The results in Fig. 6 complement those in Fig. 5 and together they show that for values of k_R of 200 and 400 the system becomes unstable with delay values above 350 ms and 110 ms respectively.

The impact of the time delay τ_d on the frequency nadir and the time the system takes to reach it are also investigated.

[1]In an actual implementation each PV plant experiences a different time delay. However it is expected that the variations among time delays for different PV plants to be on average smaller than the considered feedback delay.

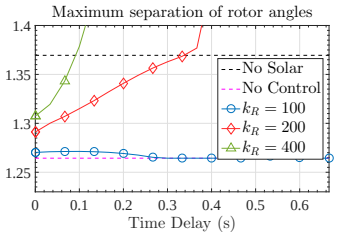

Fig. 6: Maximum rotor angle separation as a function of the time delay τ_d.

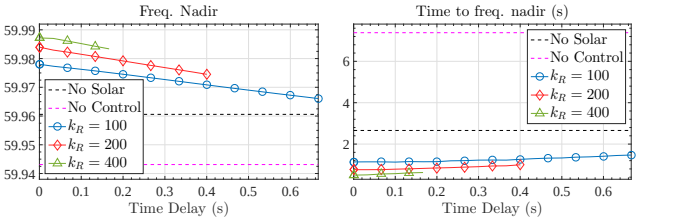

(a) Frequency Nadir as a function of the time delay τ_d.

(b) Time to Frequency Nadir as a function of the time delay τ_d.

Fig. 7: Frequency nadir and the time it takes to reach it with variations in the time delay τ_d for different gain values k_R.

Fig. 7 (a) show how increases in the time delay are reflected in the frequency nadir of the system for different values of gain k_R. These results show that the frequency nadir of the system is deteriorated with increases in τ_d. However, they also show that the decrease is not significant and in all (stable) cases considered, the CE-Droop performs better than the no control and the no solar case. In Fig. 7 (b) the impact that τ_d has on the time to frequency nadir is presented; it shows that this metric is only slightly affected by increments in the time delay. Note that Fig. 7 only presents the metrics for the cases determined to be stable according to the maximum separation of rotor angle $\Theta_{\max}$ criteria.

VI. Effect of Availability of Communication on the Frequency Response

This section studies how communication failures in CE-Droop affect the primary frequency response of the system. To this end, it is assumed that the global frequency is calculated by a centralized entity and then transmitted to each of the PV plants. The reaction of a PV plant after a communication failure is to maintain its power level until the transfer of information is restored. This action was designed such that information losses do not cause major jumps in the power levels of solar plants. To simulate communication failures, each PV plant independently determines (at a rate of 16 Hz) with a probability, whether the system frequency information has been correctly received. The probability of a successful transfer of information is termed communication availability (or availability). The results presented in this section were obtained by setting the droop gain k_R to 200 and the communications delay τ_d as 0.

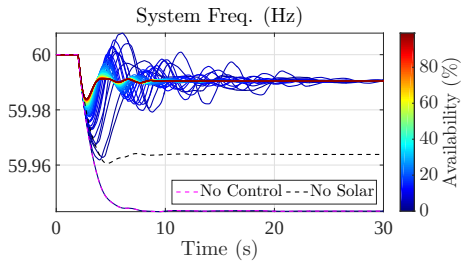

Fig. 8: Frequency response of the system as affected by different availability levels.

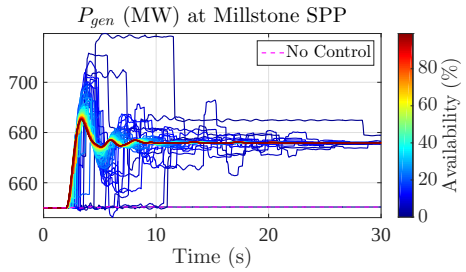

Fig. 9: Power produced by the Millstone power plant as affected by different availability levels.

A. *Effect of availability levels*

Fig. 8 shows the frequency response of the system for availability levels ranging from 1 to 99%. Note that only one realization is shown for each availability level. These results show that the response of the system is similar for availability values higher than 40%; for availability levels below this value, however, the frequency response of the system starts presenting non negligible variations and notably some oscillatory behavior appears. Fig. 9 show the active power injected by the PV plant at the Millstone Bus in the New England region of the system for the same availability levels of 1 to 99%. It is observed that for low availability levels the power output of this PV remains constant for longer periods of time as expected.

Fig. 10 shows both the frequency nadir and the time to frequency nadir of the system as affected by different availability levels (for only one realization of each level). The result in these figures show that the benefits stemming from enabling CE-Droop in solar PV plants are affected strongly for low availability levels, i.e. the frequency nadir starts decreasing and the time to reach it increasing with lower availability.

B. *Multiple Realizations of Different Availability Levels*

The results of the previous section are only qualitatively informative of the effect of availability on the frequency response of the system because they were obtained with only one realization per availability level. To capture more adequately the effect that a certain level of availability has on the response of the system, multiple simulations need to be performed (for the same level) as each simulation is different from each other because of the randomness involved in communication failures. In this section, the results of Monte

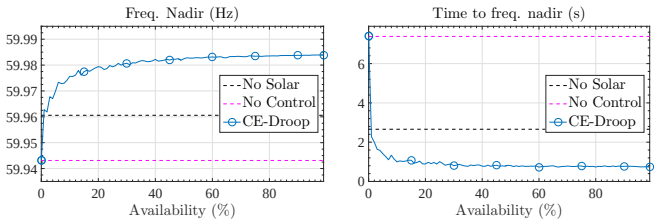

(a) Frequency Nadir as affected by different availability levels.

(b) Time to Frequency Nadir as affected by communications' availability.

Fig. 10: Frequency nadir and the time to frequency nadir as affected by different availability levels.

Carlo simulations for availability levels of 99%, 75%, 25%, and 1% are presented. Each set of simulations is composed of fifty realizations. Fig. 11 shows the frequency response of the system for each of the fifty realizations of the mentioned availability levels. These results show that for the availability levels of 99 % and 75 %, the frequency response of the system to the loss of generation event is almost unaffected by communications interruptions; that is, the variations between different simulations for a given level of availability are negligible. For the 25% availability level, some differences can be observed in the frequency response of the system as shown in Fig. 11c. For the 1% of availability level, the response of the system for each realization is very different as observed in Fig. 11d.

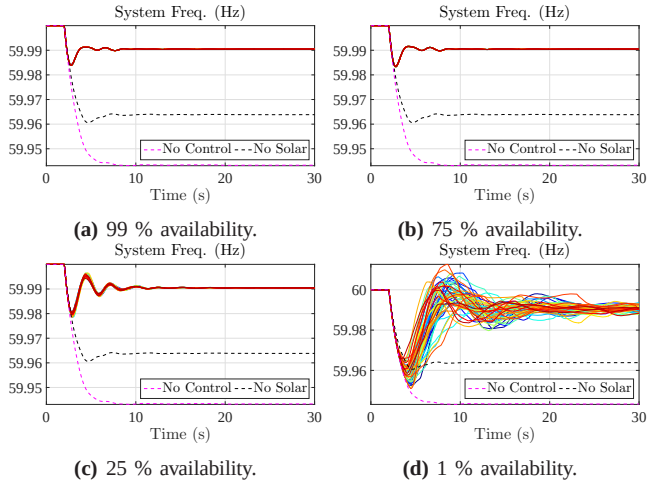

(a) 99 % availability.

(b) 75 % availability.

(c) 25 % availability.

(d) 1 % availability.

Fig. 11: Fifty realizations of the frequency response of the system at four different availability levels.

Figs. 12 and 13 present respectively the frequency nadir and the time to frequency nadir for each realization into histograms for each availability level. For consistency, the bin range and width is fixed for each of the plots. These results quantify the simulations in Fig. 11 and confirm the observations made in Section VI-A. They show that for higher levels of availability, f_N and t_{fN} are unaffected by the sporadic interruptions in communications. At 25% of availability, these results show that some variances in these metrics start appearing and that at 1% availability these variances are greatly increased. It is also

worth noting that the mean value of f_N and t_{fN} are affected negatively (which means lower values for f_N and larger values for t_{fN}) when the availability decreases.

Together, the results in Figs. 11, 12, 13 show that the proposed CE-droop is very robust to interruptions in the transfer of information. They show that communication values only affect the performance of CE-Droop for availability values below 25% (or communication failures above 75%). This result can be partially explained by the fact that the dynamics of the system are much slower than the 16 Hz polling rate that determines communication failures. It is worth mentioning that the failures in communication considered in this paper are independent for each of the PV plants in the system and it is very unlikely that all PV plants (or most of them) are affected by interruptions on the information transfer at the same time (particularly for the low probability levels). This feature could partially explain why the proposed approach performs that well for low availability levels.

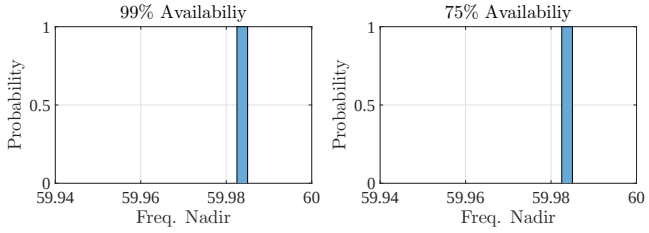

(a) 99 % availability. **(b)** 75 % availability.

(c) 25 % availability. **(d)** 1 % availability.

Fig. 12: Histogram of the frequency nadir using 50 instances for different availability levels.

VII. Conclusions

This paper proposes a new approach of implementing droop control for converter interfaced generation to enhance the primary frequency regulation in power systems. The novelty consists of using global frequency as a feedback signal instead of the traditionally used local signal. The paper analyzes the benefits and drawbacks of using such type of signal compared to the local one. Because the proposed method requires the transfer of information, the paper analyzes how the performance of the proposed approach is impacted by both communication latencies and availability. The results indicate that for different droop gains, the proposed approach performs better than the conventional approach of using local feedback. The results also show that excessive time delays, above 400 ms, can affect the performance of the controller and even cause system instabilities. The paper also finds that the proposed

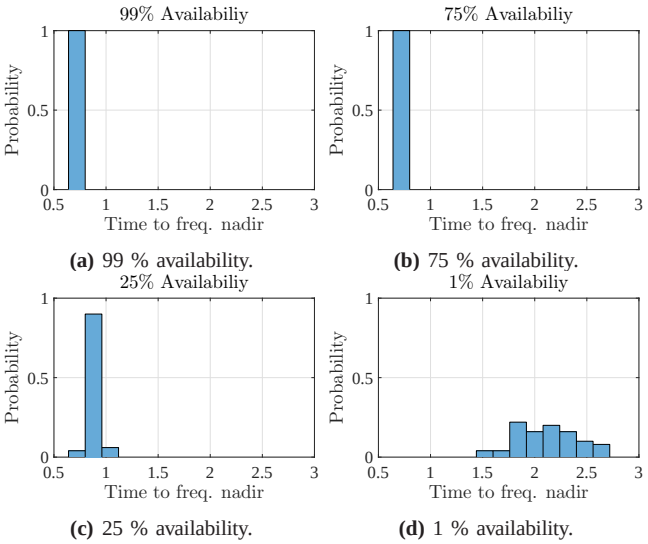

(a) 99 % availability. **(b)** 75 % availability.

(c) 25 % availability. **(d)** 1 % availability.

Fig. 13: Histogram of the time to frequency nadir using 50 instances for different availability levels.

controller is very robust to communication failures and only is affected when communications are available below 25% of the time which is a failure rate of over 75%.

References

[1] *NERC IVGTF Task 2.4 Report- Operating Practices, Procedures, and Tools*, NERC, Princeton, NJ, Mar. 2011.

[2] A. Mullane and M. O'Malley, "The inertial response of induction-machine-based wind turbines," *IEEE Trans. Power Syst.*, vol. 20, no. 3, pp. 1496–1503, Aug. 2005.

[3] F. Wilches-Bernal, J. H. Chow, and J. J. Sanchez-Gasca, "A fundamental study of applying wind turbines for power system frequency control," *IEEE Trans. Power Syst.*, vol. 31, no. 2, pp. 1496–1505, 2016.

[4] S. Eftekharnejad, V. Vittal, G. T. Heydt, B. Keel, and J. Loehr, "Impact of increased penetration of photovoltaic generation on power systems," *IEEE Trans. Power Syst.*, vol. 28, no. 2, pp. 893–901, 2013.

[5] F. Wilches-Bernal, C. Lackner, and J. H. Chow, "Power system controllability through nontraditional generation," in *55th Annu. Conf. on Decision and Control (CDC), 2016 IEEE*, Las Vegas, NV, 2016, pp. 702–708.

[6] J. Aho, A. Buckspan, J. Laks, P. Fleming, Y. Jeong, F. Dunne, M. Churchfield, L. Pao, and K. Johnson, "A tutorial of wind turbine control for supporting grid frequency through active power control," in *Amer. Control Conf. (ACC), 2012*, Montreal, QC, 2012, pp. 3120–3131.

[7] R. G. De Almeida and J. A. Peças Lopes, "Participation of doubly fed induction wind generators in system frequency regulation," *IEEE Trans. Power Syst.*, vol. 22, no. 3, pp. 944–950, Aug. 2007.

[8] J. Aho, A. Buckspan, L. Pao, P. Fleming *et al.*, "An active power control system for wind turbines capable of primary and secondary frequency control for supporting grid reliability," in *Proc. 51st AIAA Aerospace Sciences Meeting Including the New Horizons Forum and Aerospace Expo.*, 2013.

[9] R. H. Byrne, R. J. Concepcion, J. Neely, F. Wilches-Bernal, R. T. Elliott, O. Lavrova, and J. E. Quiroz, "Small signal stability of the western north american power grid with high penetrations of renewable generation," in *Photovoltaic Specialists Conference (PVSC), 2016 IEEE 43rd*. IEEE, 2016, pp. 1784–1789.

[10] R. Concepcion, F. Wilches-Bernal, and R. H. Byrne, "Effects of communication latency and availability on synthetic inertia," in *Innovative Smart Grid Technologies, ISGT 2017*, Washington, DC, 2017, pp. 1–6.

[11] J.C. Neely *et al.*, "Damping of inter-area oscillations using energy storage," in *Power and Energy Soc. General Meeting, 2013 IEEE*, Vancouver, BC, 2013, pp. 1–5.